Light scattering from an atomic gas under conditions of quantum degeneracy

V. M. Porozova,[1] L. V. Gerasimov,[2] M. D. Havey,[3] and D. V. Kupriyanov[1,*]

[1]*Department of Theoretical Physics, St. Petersburg State Polytechnic University, 195251 St. Petersburg, Russia*
[2]*Faculty of Physics, M.V. Lomonosov Moscow State University, Leninskiye Gory 1-2, 119991 Moscow, Russia*
[3]*Department of Physics, Old Dominion University, Norfolk, Virginia 23529, USA*

Elastic light scattering from a macroscopic atomic sample existing in the Bose-Einstein condensate phase reveals a unique physical configuration of interacting light and matter waves. However, the joint coherent dynamics of the optical excitation induced by an incident photon is influenced by the presence of incoherent scattering channels. For a sample of sufficient length the excitation transports as a polariton wave and the propagation Green's function obeys the scattering equation which we derive. The polariton dynamics could be tracked in the outgoing channel of the scattered photon as we show via numerical solution of the scattering equation for one-dimensional geometry. The results are analyzed and compared with predictions of the conventional macroscopic Maxwell theory for light scattering from a nondegenerate atomic sample of the same density and size.

I. INTRODUCTION

Light scattering from ultracold atomic systems existing under conditions of quantum degeneracy is a challenging and intriguing issue for both quantum optics and atomic physics. Together, investigation of these combined fields is practically important for developing various quantum interface protocols between light and matter subsystems. Although light scattering from either degenerate Bose or Fermi gases is of strong interest, we consider in the current context the degenerate Bose gas only, which is most typical for alkali-metal systems. The superposed light and matter wave propagating as a single quantum optical excitation through a Bose-Einstein condensate (BEC) phase was predicted in [1] even before the BEC had been created in the laboratory. Since the successful experimental realizations of BEC in alkali-metal systems reported in [2,3], evident signatures of cooperative dynamics in light scattering from the condensate have been observed in a series of experiments. These include manifestation of superradiant behavior of Rayleigh scattering in [4–6], formation of superfluid vortices induced by coherent optical processes in [7–9] and spin vortices in [10], and optical control of the BEC phase transition with Faraday imaging technique in [11]. The strong coherent coupling of light with a sample led to the condensate fragmentation [4–6] and an explanation of such a quite nontrivial optomechanical effect has been attempted in [5] in terms of a Kapitza-Dirac diffraction phenomenon.

The above experiments have encouraged development of theoretical insights towards a deeper understanding and precise description of light scattering under conditions of quantum degeneracy and from BEC in particular. The basic concept of a master equation for the order parameter suggests a relevant approach based on time-dependent generalization of the nonlinear Schrödinger (Gross-Pitaevskii) equation [12–14].

The coherent effects of conversion of either linear or angular momentum from light to the condensate are associated with a stimulated Raman process mediating the dynamics of the order parameter [9,14]. The superradiant properties of the Rayleigh scattering, observed in a BEC, was explained by making use of the effective Hamiltonian approach via the mechanism of cooperative emission induced by a coherent classical pump in [15–19].

In the present report we focus on a microscopic quantum theory of a single-photon scattering towards an *ab initio* description of elastic light scattering from a macroscopic atomic sample existing in the quantum degenerate BEC phase. Following the second quantized formalism, Bogoliubov theory [20], and the Gross-Pitaevskii model [21,22], we introduce a set of coupled and closed diagram equations for the polariton propagator contributing to the *T* matrix and scattering amplitude. Under conditions of bosonic quantum degeneracy for atoms, we follow important density corrections to the quasienergy structure caused by static interactions and radiation losses associated with incoherent scattering. We aim to test the validity of the conventional macroscopic Maxwell description for the quantum degenerate gas and to follow possible deviations with light scattering from a nondegenerate atomic sample of the same density and size.

This paper is organized as follows. In Sec. II we develop our general theoretical framework of light scattering from a quantum degenerate atomic gas. This represents a detailed elaboration of the sketch presented in an earlier work [23]. In Sec. III we derive the basic scattering equation via the Feynman diagram method (briefly explained in Appendix A) and discuss general properties of the Green's function (polariton propagator) responsible for transporting an optical excitation in a BEC sample. In Sec. IV we present the results of our numerical simulations for light scattering in a one-dimensional geometry; the calculational scheme is detailed in Appendix B. In Sec. V we make some concluding remarks.

*kupr@dk11578.spb.edu

II. SCATTERING PROBLEM UNDER CONDITIONS OF QUANTUM DEGENERACY

The amplitude of a photon scattered by a quantum system is given by the T matrix

$$\hat{T}(E) = \hat{V} + \hat{V}\frac{1}{E - \hat{H}}\hat{V}. \tag{2.1}$$

In this definition, $\hat{H}$ is the Hamiltonian of the quantum system. It is built from an unperturbed part $\hat{H}_0$ and an interaction term $\hat{V}$ such that $\hat{H} = \hat{H}_0 + \hat{V}$.

The differential cross section is expressed in terms of the scattering amplitude, given by the applicable T-matrix element, which is a function of the initial energy E_i:

$$d\sigma_{i \to f} = \frac{\mathcal{V}^2 \omega'^2}{\hbar^2 c^4 (2\pi)^2}|T_{g'\mathbf{e}'\mathbf{k}';g\mathbf{e}\mathbf{k}}(E_i + i0)|^2 d\Omega. \tag{2.2}$$

An initial state $|i\rangle = |g;\mathbf{e},\mathbf{k}\rangle$ is defined by the incoming photon wave vector $\mathbf{k}$, frequency $\omega \equiv \omega_k = ck$, polarization vector $\mathbf{e}$, and the quantum numbers of the scattering system $|g\rangle$. In the case of a collection of atoms, under strict conditions of quantum degeneracy, $|g\rangle = |\text{BEC}\rangle^N$ initially describes a collective state of N atoms in the BEC phase. The final state $|f\rangle = |g';\mathbf{e}',\mathbf{k}'\rangle$ is specified by a similar set of quantum numbers, with the exception that $|g'\rangle$ can exist in a disturbed condensate state for inelastic channels, and the solid angle Ω is directed along the wave vector of the outgoing photon $\mathbf{k}'$. The quantization volume $\mathcal{V}$ appearing in the differential cross section is required by the second quantized description of the interaction operators for the quantum degenerate system in the basis of plane-wave modes for the scattering photon and the atoms. The total cross section can be obtained from the diagonal T-matrix element:

$$\sigma_{\text{tot}} = -\frac{2\mathcal{V}}{\hbar c}\text{Im}T_{ii}(E_i + i0). \tag{2.3}$$

Then the cross section can be evaluated via calculation of one T-matrix element for the elastic forward scattering channel.

For a weakly interacting quantum gas (see the comment at the end of this section) the interaction term $\hat{V}$ in Eq. (2.1) can be taken in the dipole long-wavelength approximation [24–26], which is given by

$$\hat{V} = -\sum_n \int d^3 r \left[d^\mu_{nm}\hat{E}_\mu(\mathbf{r})\hat{\Psi}^\dagger_n(\mathbf{r})\hat{\Psi}_m(\mathbf{r}) + \text{H.c.}\right], \tag{2.4}$$

where d^μ_{nm} is the matrix element of the μth vector component of an atomic dipole moment and n and m respectively specify the excited and ground states of the atom. In addition, $\hat{E}_\mu(\mathbf{r})$ is the μth vector component of the electric-field operator and for the sake of generality we use covariant or contravariant notation for the vector and tensor indices. The operators $\hat{\Psi}_m(\mathbf{r})$ and $\hat{\Psi}^\dagger_n(\mathbf{r})$ are the second quantized annihilation and creation operators of an atom at position $\mathbf{r}$ respectively in the ground and excited states. We will further consider a BEC consisting of the simplest two-level atoms with a ^1S ground state and ^1P excited state such that quantum numbers $n = 0,\pm 1$ and $m = 0$ respectively denote the single-atom angular momentum projection of the excited and ground states.

In accordance with the general concept of quantum degeneracy for the system ground state existing in the BEC phase at zero temperature (see [25]), we accept that

$$\hat{\Psi}_0(\mathbf{r})|\text{BEC}\rangle^N = \Xi(\mathbf{r})|\text{BEC}\rangle^{N-1}, \tag{2.5}$$

where $\Xi(\mathbf{r})$ is the order parameter (often termed the wave function) of the condensate. We consider the BEC as a macroscopic object such that the order parameter is insensitive to any small variation of the number of particles in the condensate. Then the scattering amplitude, expressed by on-shell T-matrix elements contributing to Eqs. (2.2) and (2.3) for the scattering of an incident photon of frequency ω to the outgoing photon of frequency ω', is given by

$$\begin{aligned}
T_{fi}(E) &= \frac{2\pi\hbar(\omega'\omega)^{1/2}}{\mathcal{V}}\iint d^3r' d^3r \sum_{n',n} \\
&\times (\mathbf{d}\cdot\mathbf{e}')^*_{n'0}(\mathbf{d}\cdot\mathbf{e})_{0n}e^{-i\mathbf{k}'\mathbf{r}'+i\mathbf{k}\mathbf{r}}\;\Xi^*(\mathbf{r}')\Xi(\mathbf{r}) \\
&\times \left(-\frac{i}{\hbar}\right)\int_0^\infty dt\, e^{(i/\hbar)(E-E_0^{N-1}+i0)t}iG_{n'n}(\mathbf{r}',t;\mathbf{r},0),
\end{aligned} \tag{2.6}$$

where E_0^{N-1} is the initial energy of the condensate consisting of $N-1$ particles. The internal dynamics of the scattering process is described by a single optical excitation evolving in the condensate

$$iG_{n'n}(\mathbf{r}',t';\mathbf{r},t) = \langle\text{BEC}|T\Psi_{n'}(\mathbf{r}';t')\Psi^\dagger_n(\mathbf{r};t)|\text{BEC}\rangle^{N-1} \tag{2.7}$$

with projection onto the product of condensate and field vacuum states such that entirely

$$|\text{BEC}\rangle^{N-1} \equiv |\text{BEC}\rangle^{N-1}_{\text{atoms}}|0\rangle_{\text{field}}. \tag{2.8}$$

Equation (2.7) defines the time-ordered causal Green's function (propagator) associated with the polaritonic quasiparticle excitation superposed between the field and atom. The excitation propagates through a condensate consisting of $N-1$ particles. The operators contributing to the polariton propagator are the original atomic operators transformed in the Heisenberg representation and dressed by the interaction process. In the element of the T matrix of the form (2.6), the outer operators $\hat{V}$ in their basic definition (2.1) are revealed in the rotating-wave approximation (RWA). Such an assumption is valid since we are interested in nearly resonant scattering when both ω and ω' are close to the atomic transition frequency ω_0.

The Green's function (2.7), rewritten in the interaction representation, can be expanded in the perturbation theory series

$$\begin{aligned}
iG_{n'n}&(\mathbf{r}',t';\mathbf{r},t) \\
&= \langle\text{BEC}|\hat{S}^{-1}T[\Psi^{(0)}_{n'}(\mathbf{r}';t')\Psi^{(0)\dagger}_n(\mathbf{r};t)\hat{S}]|\text{BEC}\rangle^{N-1} \\
&= \langle\text{BEC}|T[\Psi^{(0)}_{n'}(\mathbf{r}';t')\Psi^{(0)\dagger}_n(\mathbf{r};t)\hat{S}]|\text{BEC}\rangle^{N-1}, \tag{2.9}
\end{aligned}$$

where in the interaction representation the Ψ operator is superscripted by the index (0). We consider that the condensate itself is a stable system, which should not be modified by the interaction (2.4) without its advanced perturbation by an incoming photon. This should be justified by the requirement that the evolution operator

$$\hat{S} = T\exp\left[-\frac{i}{\hbar}\int_{-\infty}^\infty \hat{V}^{(0)}(t)e^{-0|t|}\right] \tag{2.10}$$

does not change the BEC state such that $\hat{S}|\text{BEC}\rangle^{N-1} = |\text{BEC}\rangle^{N-1}$. Although this requirement seems to be accepted in assumptions of the RWA, let us make an important remark concerning its applicability.

The condensate, considered as a physical object, is not an ideal gas. The small but physically important difference $E_0^N - E_0^{N-1} = \varepsilon_0 \equiv \mu_c + E_0$ gives a binding energy for adding a particle into an atomic ensemble, which incorporates the chemical potential μ_c and the internal ground-state energy E_0 of a single atom. The latter could be set to zero, but in our derivation it is convenient to leave E_0 as a physical parameter. For the quantum degenerate gas, consisting of not extremely dense and weakly interacting atoms and fairly described in the framework of the Gross-Pitaevskii model [21,22], the inequality

$$\mu_c \lesssim \frac{\hbar^2 k_0^2}{2m_A} \ll \hbar\gamma \tag{2.11}$$

is fulfilled, where $k_0 \equiv \lambdabar_0^{-1}$ is wave number for a resonant photon, m_A is the atomic mass, and γ is the natural spontaneous decay rate for the upper state of the atom. In accordance with the model (see [25]), the chemical potential for a homogeneous BEC is given by

$$\mu_c = n_0 \int d^3r \, U(r) > 0, \tag{2.12}$$

where $U(r)$ is an interaction potential in the system of two atoms and n_0 is the atomic density. The subtle point is that the interaction $U(r)$ incorporates both the short-range repulsive part and the long-range attractive dipole-dipole polarization interactions. The latter is also known as the van der Waals interaction and the related asymptotic behavior of the potential $U(r)$ is constructed in the second order of the same Hamiltonian (2.4) but keeping the terms beyond and alternative to the RWA concept.

The conflicting situation with double accounting of the interaction Hamiltonian (2.4) can be resolved once we pay attention to the fact that the van der Waals interaction is meaningful on a distance of an atomic scale $r \sim O(1)a_0$, where a_0 is the Bohr radius, but the optical coupling experiences the distances $r \sim \lambdabar_0 \gg a_0$. That means that there is no intersection in the diagram representation of $U(r)$ with those which are induced by the evolution operator (2.10) and which couple a pair of distant atoms where one is always excited. In this case the evolution operator (2.9) indeed does not affect the condensate state and the second line in Eq. (2.9) is valid beyond the restrictions of the RWA approach since the internal interaction in the atomic ensemble is weak and can be safely separated from the optical excitation dynamics mediated by the scattering process.

The inequality (2.11) provides us with the chemical potential as the smallest parameter of the theory and is fulfilled up to the densities $n_0 \lambdabar_0^3 \gtrsim 1$. This is a typical condition when considering a condensate consisting of alkali-metal atoms. From the physical point of view that means that we consider the BEC in conditions close to an ideal gas and assume that the matrix elements in (2.4), as well as the atomic energy structure in the perturbation theory expansion, is the same as for independent atoms. Nevertheless, we do not ignore the

gas nonideality and the interatomic interaction $U(r)$ in the ground state as it is crucially important for proper description of the general behavior of the order parameter $\Xi = \Xi(\mathbf{r},t)$ under the framework of the Gross-Pitaevskii model including superfluidity as the main macroscopic quantum property of the condensate. In its main approximations, our consideration is applicable up to the bound of $\mu_c \lesssim \hbar\gamma$.

III. DYNAMICS OF THE OPTICAL EXCITATION IN THE CONDENSATE

A. Diagrammatic representation

The polariton propagator (2.9) can be expanded in the perturbation theory series and the appearing terms can be regrouped with the Feynman diagram method. The basic elements and definitions are given in Appendix A. Since the considered interaction processes are primarily developing in near-resonance conditions, we follow the RWA approach and keep the leading expansion terms. Eventually, the polariton propagator can be constructed as a dressed Green's function of an excited atom and obeys the Dyson-type diagram equation
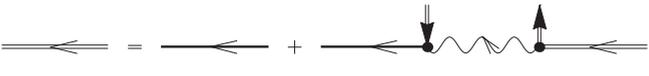
$$\tag{3.1}$$

where it is depicted as a straight double line. This corresponds to the fact that the original atomic propagator is assumed dressed by all interaction processes. The ingoing and outgoing vertical arrows provide an image of the order parameter and form the self-energy part responsible for coherent conversion of the excitation between the field, in which the free dynamics is expressed by an undressed wavy line, and an atom subsequently recovered in the condensate phase. Consistent with this diagram equation, the above coherent process partly degrades because of interaction with the vacuum modes when the excited atom emits a photon spontaneously and escapes coherent dynamics, propagating through the condensate as a simple spectator.

The latter process contributes in (3.1) with an incomplete polariton propagator, which is illustrated by a straight solid line in the diagrams and obeys the Dyson-type equation

$$\tag{3.2}$$

which should be considered together with the equation for the dressed field propagator

$$\tag{3.3}$$

These two diagram equations are mutually closed and reproduce the self-consistent dynamics of an atomic dipole interacting with its environment, similar to the conditions in a typical disordered atomic gas. Indeed, any optical excitation created from the condensate has a chance to be incoherently reemitted into the vacuum modes and transfer the atom, emitting such a photon, out of the condensate phase. These circumstances are

described by the incomplete polariton propagator (3.2) having a similar diagrammatic representation as atomic excitation in a disordered gas. Such incoherent scattering induces losses and leads to degradation of coherent dynamics supported by the self-energy operator in Eq. (3.1). In a natural optical association this process introduces the dielectric permittivity constructed in a way similar to that of a disordered atomic gas of the same density.

B. Incoherent losses and the dielectric permittivity of the condensate

The self-energy part in (3.3) (polarization operator) emphasizes the coherent structure of the matter state considered in conditions of quantum degeneracy. Nevertheless, for an infinite, locally homogeneous isotropic medium, which physically requires that the sample size and inhomogeneity scale of the order parameter $\Xi(\mathbf{r})$ would be comparable to or longer than the radiation wavelength, the solution of Eq. (3.3) is expected to be similar to the case of a disordered atomic gas of the same density. Indeed, both vertices in the self-energy part of Eq. (3.3) are linked by the propagator (3.2) in which the respective resonant excitation degrades on a time scale of natural decay when the excited atom can drift a distance much less than its radiation wavelength. Thus both vertices are taken in proximal spatial points such that the order parameter actually contributes to Eq. (3.2) as the local atomic density $n_0(\mathbf{r}) = |\Xi(\mathbf{r})|^2$. With this simplification we can construct solutions of Eqs. (3.2) and (3.3) as for an infinite, homogeneous isotropic medium in closed analytical form and compare the result with the similar performance of an incoherent scattering process developing in a disordered atomic gas.

1. Analytical performance

For the sake of convenience and for further derivation we switch the primed and unprimed arguments and indices in the notation of the Green's functions [see, for example, Eq. (2.9) and our definitions of the undressed functions in Appendix A]. In stationary and homogeneous conditions these functions depend only on the difference between their spatial and time arguments. Then we can make a Fourier transform for the dressed Green's functions, constructed by the diagram method, and define

$$
\mathcal{D}_{\mu\mu'}^{(E)}(\mathbf{k},\omega)
$$
$$
= \int d^3R \int_{-\infty}^{\infty} d\tau \, e^{i\omega\tau - i\mathbf{k}\cdot\mathbf{R}} \mathcal{D}_{\mu\mu'}^{(E)}(\mathbf{R},\tau)\Big|_{\substack{\mathbf{R}=\mathbf{r}-\mathbf{r}' \\ \tau=t-t'}} \quad (3.4)
$$

for the photon propagator, fulfilling Eq. (3.3), and

$$
G_{nn'}^{(\gamma)}(\mathbf{p},E)
$$
$$
= \int d^3R \int_{-\infty}^{\infty} d\tau \, e^{(i/\hbar)E\tau - (i/\hbar)\mathbf{p}\cdot\mathbf{R}} G_{nn'}^{(\gamma)}(\mathbf{R},\tau)\Big|_{\substack{\mathbf{R}=\mathbf{r}-\mathbf{r}' \\ \tau=t-t'}}
$$
$$
(3.5)
$$

for the incomplete polariton propagator, fulfilling Eq. (3.2). The superscript γ is added to associate such a propagator with excitation dynamics mediated by spontaneous scattering processes. In the representation (3.4) we assume the dressed

positive-frequency component of the vacuum Green's function (A4) with $\omega > 0$ and the equivalence between the causal and retarded-type definitions for this case.

In the Fourier representation Eq. (3.3) can be straightforwardly resolved with respect to the incomplete polariton propagator

$$
\mathcal{D}_{\mu\mu'}^{(E)}(\mathbf{k},\omega) = -\frac{4\pi\hbar\omega^2}{\omega_k^2 - \epsilon(k,\omega)\omega^2}\left[\delta_{\mu\mu'} - c^2\frac{k_{\mu'}k_\mu}{\epsilon(k,\omega)\omega^2}\right]
$$
$$
\approx -\frac{4\pi\hbar\omega^2}{\omega_k^2 - \epsilon(\omega)\omega^2}\left[\delta_{\mu\mu'} - c^2\frac{k_{\mu'}k_\mu}{\epsilon(\omega)\omega^2}\right], \quad (3.6)
$$

where

$$
\epsilon(k,\omega) = 1 - \frac{4\pi}{\hbar}d_0^2 n_0 G^{(\gamma)}(\hbar k, \hbar\omega + \varepsilon_0). \quad (3.7)
$$

Here d_0 is the modulus of the transition dipole moment (the same for all the transitions), $n_0 = |\Xi|^2 = \text{const}$ is the density of atoms, and for an isotropic medium with a degenerate excited state ($E_n = \text{const}_n$) we have

$$
G_{nn'}^{(\gamma)}(\mathbf{p},E) = \delta_{nn'}G^{(\gamma)}(p,E). \quad (3.8)
$$

Taking into account the inequality (2.11), we expect a negligible deviation in (3.7) from the limit of immobile atoms and approximate $\epsilon(k,\omega) \approx \epsilon(0,\omega) \equiv \epsilon(\omega)$, which justifies the second line in Eq. (3.6). Equation (3.6) (as well as similar tensor relations found later in the paper) is performed for Cartesian components $\mu,\mu' = x,y,z$, but for the case of spherical components $\mu,\mu' = 0,\pm 1$ one has to change $\delta_{\mu\mu'} \to g_{\mu\mu'} = (-1)^\mu \delta_{\mu,-\mu'}$.

The obtained result looks similar to that of a conventional medium beyond quantum degeneracy. As we can see, with reference to [25], such a type of photon Green's function in a medium can be associated with a fundamental solution of the macroscopic Maxwell equations where $\epsilon(\omega)$ is the dielectric permittivity of the medium. However, in the case of quantum degeneracy the excitations in both the field and matter subsystems, i.e., the photon and the excited atom, transport through the sample in a superposed polariton mode, as suggested by the complete graph equation (3.1). Although the association with a conventional medium is not intrinsically consistent, we call $\epsilon(\omega)$ a dielectric permittivity of the condensate, keeping in mind in such an analogy that it is constructed involving only the contribution of excitations over the condensate created in the incoherent scattering process.

Equation (3.2), decoded in the Fourier representation, contains the field Green's function (3.6) contributing to the self-energy part in the form of the convolution integral with an atomic propagator (see Appendix A for a clarifying comment). Since recovering the incoherent losses as well as the interaction with the quantized continuum is mostly important for nearly resonant conditions, we can expect that in the integral evaluation, the internal arguments are varied in sufficiently broad domains but located near $\omega \sim \omega_0$ and $k \sim k_0 = \omega_0/c$, where $\omega_0 = (E_n - E_0)/\hbar$ is the atomic transition frequency. Considering the field Green's function as an analytical function of detuning $\Delta = \omega - \omega_0$ in the complex half plane where $\text{Im}[\Delta] > 0$, the integral over ω (approximated as an integral over Δ in infinite limits) can be reliably reproduced by the residue at the pole point $\omega_E = (E - E_0)/\hbar$ [where $\Delta \to$

$\Delta_E = (E - E_n)/\hbar$]. In such an estimate we can safely ignore the small pole displacement associated with the Doppler shift as a negligible relativistic-type correction to the remaining integral evaluated over $\mathbf{k}$ variable.

Under these assumptions, Eq. (3.2) reads

$$\left[E - \frac{p^2}{2m_A} - E_n - \Sigma^{(\gamma)}(p,E) \right] G^{(\gamma)}(p,E) = \hbar \qquad (3.9)$$

and the self-energy part $\Sigma^{(\gamma)}(p,E)$ is expressed by the sum

$$\Sigma^{(\gamma)}(p,E) = \Sigma^{(\mathrm{st})}(p,E) + \Sigma^{(\mathrm{rad})}(p,E), \qquad (3.10)$$

where the first term is given by

$$\begin{aligned} \Sigma^{(\mathrm{st})}(p,E) &= \frac{4\pi}{3} \int \frac{d^3k}{(2\pi)^3} \frac{d_0^2}{\epsilon(k,\omega_E)} \\ &\approx \frac{4\pi}{3} \int \frac{d^3k}{(2\pi)^3} \frac{d_0^2}{\epsilon(\omega_E)} \end{aligned} \qquad (3.11)$$

and can be associated with the interaction of the dipole with its own field in the environment of the over-condensate component, created in the incoherent excitation process. The second term is given by

$$\begin{aligned} \Sigma^{(\mathrm{rad})}(p,E) &= -\frac{8\pi}{3} d_0^2 \int \frac{d^3k}{(2\pi)^3} \frac{\omega_E^2}{c^2 k^2 - \epsilon(k,\omega_E)\omega_E^2} \\ &\approx -\frac{8\pi}{3} d_0^2 \int \frac{d^3k}{(2\pi)^3} \frac{\omega_E^2}{c^2 k^2 - \epsilon(\omega_E)\omega_E^2} \end{aligned} \quad (3.12)$$

and reveals radiation backaction of the incoherent emission on the dipole's dynamics.

Equations (3.9)–(3.12) and (3.7) entirely construct one closed but quite complicated self-consistent equation for the incomplete propagator $G^{(\gamma)}(p,E)$, which has a nonlinear integral form. However, the equation can be essentially simplified by applying a faithful approximation, expressed by the second lines in Eqs. (3.11) and (3.12), which assumes that in Eq. (3.9) the kinetic energy term for $p \sim \hbar k_0$ is small in comparison to the self-energy part. As we have pointed out above, this is justified by the inequality (2.11). In this approximation the dielectric permittivity $\epsilon(\omega)$ and the function $G^{(\gamma)}(p,E)$ (with $p \sim \hbar k_0$) can be found in an analytical form once we resolve the problem with divergences existing in both contributions to the self-energy part (3.10).

2. Renormalization of the self-energy divergences

Let us express the contribution (3.11) in the form

$$\Sigma^{(\mathrm{st})}(p,E) \sim -\mathbf{d} \cdot \mathbf{E}^{(\mathrm{vac})}(\mathbf{0}) - \mathbf{d} \cdot [\mathbf{E}^{(\mathrm{med})}(\mathbf{0}) - \mathbf{E}^{(\mathrm{vac})}(\mathbf{0})],$$
$$(3.13)$$

where we have assumed that an atomic dipole $\mathbf{d}$ is located at the origin of the coordinate frame and the diverging integral (3.11) was converted to the dipole's infinite electric field $\mathbf{E}^{(\mathrm{med})}(\mathbf{0})$ in the medium with a dielectric constant ϵ. We also subtracted and added the same quantity existing in vacuum with $\epsilon = 1$. The vacuum term means the dipole self-action, i.e., an artificial object of the theory, which reveals the incorrectness of the dipole gauge on the distances comparable to the atomic scale. The infinite energy, associated with this term, should be incorporated into the physical energy of the excited atom as

internal energy of the pointlike dipole particle. Then the second term in Eq. (3.13) is a physical quantity showing how the dipole self-action is modified in the environment of other dipoles. One expects that the incoherent scattering is a locally cooperative process and the selected dipole is indistinguishable from other proximal dipoles responding to the driving field of an exciting photon. Then, in accordance with the arguments performed in Refs. [26–28], we can accept the standard Lorentz-Lorenz interpretation of the field and energy shift, associated with static interaction of a collection of proximal dipoles

$$\mathbf{E}^{(\mathrm{med})}(\mathbf{0}) - \mathbf{E}^{(\mathrm{vac})}(\mathbf{0}) \to \frac{4\pi}{3} n_0 \mathbf{d},$$

$$\Sigma^{(\mathrm{st})}(p,E) \to -\frac{4\pi}{3} n_0 d_0^2, \qquad (3.14)$$

where we substituted $\mathbf{d}^2 \to d_0^2$.

The second contribution (3.12) can be interpreted as an interaction with the quantized vacuum continuum manifestable via the radiation Lamb shift and spontaneous decay rate. By setting $\epsilon = 1$ the integral transforms to

$$\Sigma^{(\mathrm{vac})}(p,E) = -\frac{8\pi}{3} d_0^2 \int \frac{d^3k}{(2\pi)^3} \frac{\omega_E^2}{c^2 k^2 - \omega_E^2 - i0} \bigg|_{E \sim E_n}$$

$$\Rightarrow \hbar\Delta_L - \frac{i\hbar}{2}\gamma, \qquad (3.15)$$

where $\Delta_L \to \infty$ is the vacuum Lamb shift further renormalized and incorporated into the atomic energy E_n, dressed by interaction with the vacuum modes. The regularized integral given by the difference of (3.12) and (3.15) becomes converging and reproducible by residues at its pole points. Eventually, we arrive at the renormalization of the radiation correction to the self-energy part

$$\Sigma^{(\mathrm{rad})}(p,E) \Rightarrow -\frac{i\hbar}{2}\sqrt{\epsilon(\omega_E)}\gamma, \qquad (3.16)$$

which contains both the radiation damping and energy shift modified by the radiation coupling with the over-condensate component created by the excitation process.

3. Incomplete propagator in closed form

By substituting the renormalized self-energy parts (3.14) and (3.16) into (3.10) and (3.9) and in accordance with our definition of the dielectric permittivity given by Eq. (3.7) with $k \to 0$ we obtain the equation

$$\epsilon\left(\omega - \frac{\mu_c}{\hbar}\right) = \frac{\omega - \omega_0 - \frac{8\pi}{3\hbar} n_0 d_0^2 + \frac{i}{2}\sqrt{\epsilon(\omega)}\gamma}{\omega - \omega_0 + \frac{4\pi}{3\hbar} n_0 d_0^2 + \frac{i}{2}\sqrt{\epsilon(\omega)}\gamma}. \qquad (3.17)$$

On the left-hand side the frequency argument of the permittivity is displaced by the chemical potential μ_c. This emphasizes the fact that for a single optical excitation from the condensate the extra action is needed, which is a meaningful part of the binding energy $\varepsilon_0 = E_0 + \mu_c$ given by the chemical potential. Although in our model this displacement is rather small, it recognizes a qualitatively important extension up to the case of a strongly nonideal gas. However, by neglecting it, we obtain an equation for the dielectric permittivity identical to an atomic ensemble consisting of cold disordered and randomly distributed atomic dipoles (see Ref. [27]).

Equation (3.17) can be analytically solved and its solution can be applicable to the case of an inhomogeneous medium if the density $n_0 = n_0(\mathbf{r})$ and order parameter $\Xi(\mathbf{r})$ are varied on a spatial scale comparable to the radiation wavelength or longer. Then Eq. (3.9) suggests the approximate form in the mixed space-frequency representation

$$\left[E + \frac{\hbar^2}{2m_A}\triangle - E_n + \frac{4\pi}{3}n_0(\mathbf{r})d_0^2 \right.$$
$$\left. + \frac{i\hbar}{2}\sqrt{\epsilon(\mathbf{r},\omega_E)}\gamma \right] G^{(\gamma)}(\mathbf{r},\mathbf{r}';E) = \hbar\delta(\mathbf{r}-\mathbf{r}'), \quad (3.18)$$

where we parametrized the dielectric constant $\epsilon = \epsilon(\mathbf{r},\omega)$ by its spatial dependence. Indeed, in this equation $G^{(\gamma)}(\mathbf{r},\mathbf{r}';E)$, considered as a function of $\mathbf{r} - \mathbf{r}'$, transports a single-photon excitation, created from the immobile condensate, from point $\mathbf{r}'$ to point $\mathbf{r}$, which degrades on a spatial scale sufficiently less than $\lambdabar_0 = k_0^{-1}$. Thus Eq. (3.18) accepts only proximal spatial arguments $\mathbf{r} \sim \mathbf{r}' \sim (\mathbf{r}+\mathbf{r}')/2$, where $n_0 = n_0(\mathbf{r})$ is approximately constant.

We have constructed the *incomplete* polariton propagator (3.2) in a form that is similar to the complete excited-state propagator of a single atom in a disordered atomic gas of the same density. Such an analogy, emphasizing the similarity in spontaneous scattering from both systems, was expectable and prefaced this part of our derivation. Nevertheless, as was pointed out above, the analogy is not so straightforward and in the conditions beyond the Gross-Pitaevskii model (i.e., for a nonideal quantum gas with strong internal coupling) it could appear as an important deviation in the description of such physically different systems.

C. Complete polariton propagator

By decoding the diagram equation (3.1) for the complete polariton propagator we extend spontaneous dynamics, described by Eq. (3.18), by involving the process of coherent conversion of the excitation between the field and condensate

$$\left[E + \frac{\hbar^2}{2m_A}\triangle - E_n + \frac{4\pi}{3}n_0(\mathbf{r})d_0^2 \right.$$
$$\left. + \frac{i\hbar}{2}\sqrt{\epsilon(\mathbf{r},\omega_E)}\gamma \right] G_{nn'}(\mathbf{r},\mathbf{r}';E)$$
$$- \sum_{n''}\int d^3r''\, \Sigma_{nn''}^{(c)}(\mathbf{r},\mathbf{r}'';E)\, G_{n''n'}(\mathbf{r}'',\mathbf{r}';E)$$
$$= \hbar\delta_{nn'}\delta(\mathbf{r}-\mathbf{r}'). \quad (3.19)$$

The kernel of the respective integral self-energy operator (simplifying the argument superscripted with a double prime to a single prime) is given by

$$\Sigma_{nn'}^{(c)}(\mathbf{r},\mathbf{r}';E) = \frac{1}{\hbar}\sum_{\mu\mu'}\Xi(\mathbf{r})\Xi^*(\mathbf{r}')\,d_{n0}^{\mu}d_{0n'}^{\mu'}$$
$$\times D_{\mu\mu'}^{(E)}\left(\mathbf{r}-\mathbf{r}',\omega_E-\frac{\mu_c}{\hbar}\right), \quad (3.20)$$

where the vacuum field Green's function, expressed as the wavy line in the diagram equation (3.1) and defined by Eqs. (A1) and (A4), contributes here in the mixed space-

frequency representation

$$D_{\mu\mu'}^{(E)}(\mathbf{R};\omega) = -i\int_{-\infty}^{\infty}d\tau\, e^{i\omega\tau}\langle T E_{\mu}^{(0)}(\mathbf{r},t)E_{\mu'}^{(0)}(\mathbf{r}',t')\rangle\Big|_{\substack{\tau=t-t'\\\mathbf{R}=\mathbf{r}-\mathbf{r}'}}$$

$$= -\hbar\frac{|\omega|^3}{c^3}\left\{ i\frac{2}{3}h_0^{(1)}\left(\frac{|\omega|}{c}R\right)\delta_{\mu\nu} \right.$$
$$\left. + \left[\frac{X_\mu X_{\mu'}}{R^2} - \frac{1}{3}\delta_{\mu\mu'}\right]ih_2^{(1)}\left(\frac{|\omega|}{c}R\right) \right\}. \quad (3.21)$$

Here the averaging is over the vacuum state and $h_L^{(1)}(\cdots)$ with $L = 0,2$ are the spherical Hankel functions of the first kind.

The derived equation (3.19) traces the dynamics of a single-particle excitation in the condensate with the assumption that the order parameter, density distribution, dielectric permittivity, etc., have a smooth profile on a mesoscopic scale, similar to the conventional macroscopic Maxwell theory. It can be visualized as a Schrödinger-type equation for an excited atom propagating in space and modified by interacting with the environment. Here the kinetic energy term is actually responsible for the negligible drift of the excitation during the decay time when the transferred momentum of the polariton is limited by the value of $\hbar k_0$ in its order of magnitude. Nevertheless, the optical excitation itself can propagate through the sample with a much faster speed approaching the speed of light, which can be demonstrated via the solution of Eq. (3.19) in the limit of an infinite homogeneous medium. To show this we include below part of the discussion from our previous work [23].

Equation (3.19) can be solved in an infinite, homogeneous isotropic medium. The solution is found in the reciprocal space as a linear combination of the transverse and the longitudinal components with respect to the momentum argument. We will also take, for further calculations in this section, the internal binding energy of the condensate as weak; this means that we take the chemical potential to be negligible in comparison with characteristic spectral parameters such as the spontaneous radiative decay rate and the (much smaller) single-particle recoil energy [see (2.11)]. Then the Fourier components of the complete polariton propagator can be expanded as

$$G_{nn'}(\mathbf{p},E) = G_\parallel(p,E)\frac{p_n p_{n'}}{p^2} + G_\perp(p,E)\left[\delta_{nn'} - \frac{p_n p_{n'}}{p^2}\right], \quad (3.22)$$

where, in accordance with the selection rules for the dipole moment operators in Eq. (3.20), we link the vector indices, in the Cartesian frame, with the quasiparticle momentum $\mathbf{p}$ with quantum numbers of the atomic excited state.

The longitudinal and transverse components of the polariton propagator are given by

$$G_\parallel(p,E) = \hbar\left[E - E_n - \frac{p^2}{2m_A} - \frac{8\pi}{3}n_0 d_0^2 \right.$$
$$\left. + \frac{i\hbar}{2}\sqrt{\epsilon(\omega_E)}\gamma \right]^{-1},$$

$$G_\perp(p, E) = \hbar \left[E - E_n - \frac{p^2}{2m_A} + \frac{4\pi}{3} n_0 d_0^2 \right.$$
$$\left. + \frac{i\hbar}{2} \sqrt{\epsilon(\omega_E)}\gamma - \frac{4\pi n_0 d_0^2 \omega_E^2}{\left(\omega_E^2 - c^2 p^2/\hbar^2\right)} \right]^{-1}.$$

$$(3.23)$$

As the excitation frequency is shifted towards atomic resonance $E \to E_n$ the optical coupling shows behavior associated with that of a noncondensed disordered atomic gas. The collective dipole polarization is driven by the propagating field and the environment of nearby dipoles induces a frequency shift to the low-energy side of atomic resonance. This shift, given by $-4\pi n_0 d_0^2/3$, is the well-known static Lorentz-Lorentz shift. However, unlike a disordered gas, there is an additional frequency shift, induced by the polarization interaction with the condensate background. This is given by the last term on the right-hand side of Eq. (3.23). If we consider the quasiparticle as essentially immobile, thus having negligible momentum $p \ll \hbar\omega/c$, the dependence on E vanishes and this part of the interaction also becomes static. The transverse component of the polariton propagator then coincides with its longitudinal part such that the excitation process becomes isotropic with a positive static shift $8\pi n_0 d_0^2/3$.

The spectral behavior of the polariton propagator in the form (3.22) and (3.23) consists of two branches. One is an atom-type excitation near atomic resonance $E \sim E_n$, on which we have commented above. Another resonance exists in the transverse part of the polariton propagator and is located near the energy $E \sim E_0 + cp$, which is a pole feature of the last term in the denominator of the transverse component $G_\perp(p, E)$. This resonance describes the optical excitation propagating through the sample near the speed of light and creates the photon-type polariton branch. A detailed discussion of the spectral behavior of the polariton modes in the infinite homogeneous medium was given in [23].

In general, with an inhomogeneous configuration with the order parameter of an arbitrary profile, Eq. (3.19) accepts only a numerical solution. In the next section we present such a solution in a one-dimensional geometry and compare the results with predictions of conventional macroscopic Maxwell theory.

IV. RESULTS

Degenerate quantum gases have unique properties and are of particular interest in reduced spatial dimensionality [29,30]. This motivates us to initially consider our results for several instances of a one-dimensional model. Further, Eq. (3.19) is quite difficult for numerical solution in a general three-dimensional configuration. Below we perform the results of our numerical simulations for a one-dimensional model expressed in terms of transmission and reflection of light from a slab atomic sample, where atoms can exist either in a quantum degenerate phase or as a disordered classical gas. The considered geometries are shown in Fig. 1 for three tested configurations: a uniform slab of BEC with constant density [Fig. 1(a)], an inhomogeneous distribution parametrized by the order parameter with a cosine profile [Fig. 1(b)], and interference of two matter waves for
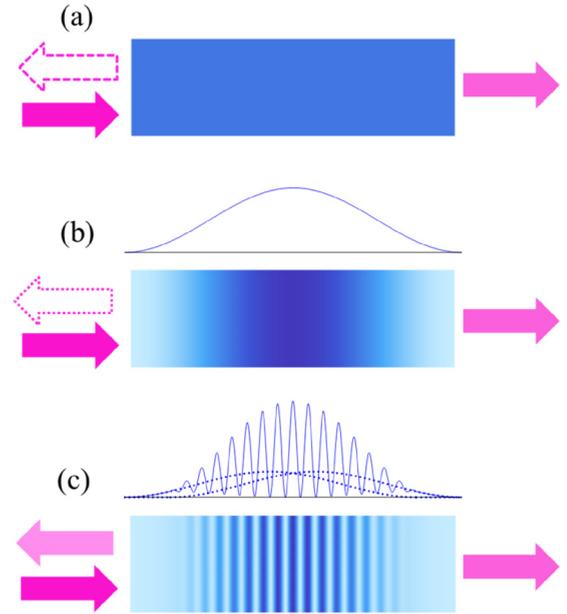

FIG. 1. Geometry of the considered one-dimensional scattering process: (a) a uniform BEC slab of depth L and with the order parameter $\Xi = \sqrt{n_0} = \mathrm{const}_z$, where n_0 is the density of atoms, (b) an inhomogeneous distribution parametrized by the order parameter $\Xi(z) = \sqrt{n_0}\cos(\pi z/L)$, and (c) interference of two matter waves created by the BEC sample (b) split in two fragments [see Eq. (4.2) and the explanation in the text].

two BEC segments counterpropagating through each other [Fig. 1(c)]. In the last case, as we show, such an internal motion of the overlapping condensate fragments can crucially modify the light scattering process.

A. Smooth profile of the order parameter

Any testable profile of the order parameter should be consistent with the physical model of the condensate and, in the case of weak internal coupling, performs as a possible solution of the Gross-Pitaevskii equation [21,22]. In the macroscopic limit any homogeneous spatial profile of the order parameter can be suggested as an example of a Thomas-Fermi-type approximate solution, for which the shape can be fitted by varying the trapping potential. This approximation works for the condensate confined by an atomic trap where the period of free oscillation is longer than $2\pi/\mu_c$, with μ_c estimated (in a homogeneous limit) by Eq. (2.12), and it is based on the priority of internal interaction. However, even in the case of an ideal gas with $\mu_c \to 0$ the order parameter of a quite general profile can be accepted as well, but in this case as the ground-state eigenfunction of the stationary single-particle Schrödinger equation in the trap potential.

As the first example let us consider the case of a homogeneous degenerate quantum gas filling a slab of depth L with the order parameter given by $\Xi = \sqrt{n_0} = \mathrm{const}_z$, which is shown in Fig. 1(a). In a one-dimensional geometry, by applying the Fourier transform, the scattering equations (3.19) can be rewritten as an infinite set of algebraic equations (see Appendix B for derivation details). The obtained system of algebraic equations can be numerically solved, which give us

the spectra of transmission $\mathscr{T}(\omega)$ and reflection $\mathscr{R}(\omega)$. The same quantities can be independently constructed via solution of the macroscopic Maxwell equations (see [31]) and are given by

$$\mathscr{T}(\omega) = \left| \frac{2\sqrt{\epsilon(\omega)}}{2\sqrt{\epsilon(\omega)}\cos\psi(\omega) - i[1 + \epsilon(\omega)]\sin\psi(\omega)} \right|^2,$$

$$\mathscr{R}(\omega) = \left| \frac{\sin[\psi(\omega)]}{\sin\left[\psi(\omega) - i\ln\frac{1-\sqrt{\epsilon(\omega)}}{1+\sqrt{\epsilon(\omega)}}\right]} \right|^2, \qquad (4.1)$$

where $\psi(\omega) = L\sqrt{\epsilon(\omega)}\omega/c$. By substituting here the dielectric permittivity (3.17) (with canceled chemical potential) we arrive at the result predicted for a macroscopic disordered gas (see [27]).

In Fig. 2 we compare the spectra of light transmission through and reflection from the condensate and disordered atomic gas of the same density $n_0\lambda_0^3 \sim 0.05$ and in the geometry of Fig. 1(a). The inset shows the dielectric permittivity given by solution of Eq. (3.17). Since an optical excitation from the condensate changes its energy, the excitation spectrum of nonideal degenerate quantum bosonic gas is redshifted from the atomic resonance by the value of the chemical potential. The shift is small and seems negligible since the condition (2.11) is normally fulfilled for any dipole-type transition and in alkali-metal systems in particular. Thus we could safely ignore this shift when constructing the susceptibility for the condensate as the solution of Eq. (3.17). Nevertheless, we leave it in our reproduction of the spectral responses since such a redshift is a physical effect and can be visible in the transmission and reflection spectra. The redshift has been observed in the transmission spectrum of a BEC consisting of helium atoms on a spectrally narrow dipole-forbidden magnetic-type transition [32].

Surprisingly, this global offset of the spectral profile is only one difference between the transmission and reflection spectra of degenerate and nondegenerate atomic gases. To demonstrate this we plotted the graphs as a function of detuning $\Delta = \omega - \tilde{\omega}_0$, where $\tilde{\omega}_0 = \omega_0 - \mu_c/\hbar$ and where we additionally displaced the spectra of a disordered gas on $\mu_c/\hbar$. We have obtained excellent, i.e., point-by-point, coincidence of degenerate and nondegenerate spectra despite the fact that they were calculated via solution of exceptionally different equations. The small deviation for reflection near its resonant point is a result of additional boundary contributions ignored in the Fourier transformation of the Laplace operator to the algebraic form of Eq. (B8) and this incorrectness, as we have verified, softens in the macroscopic limit $L/\lambda_0 \to \infty$. The reflection itself is weak but not negligible and results from the scattering from the sample edges and is enhanced by the interference effect. Such an excellent coincidence of two independent rounds of calculations clearly indicates that for light scattering from an ensemble of atoms, with a uniform density distribution, the optical response of the system is insensitive to either the classical or quantum nature of statistical averaging.

This can be confirmed by similar calculations performed for the order parameter with a trigonometric profile $\Xi(z) = \sqrt{n_0}\cos(\pi z/L)$ [in the geometry of Fig. 1(b)] and the results are shown in Fig. 3. For this case we make additional simplifica-
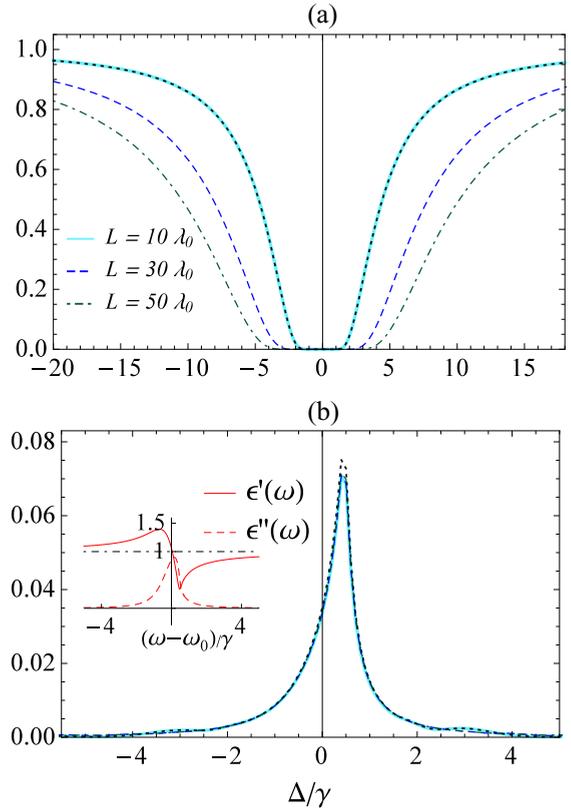

FIG. 2. Spectral dependences of (a) transmission and (b) reflection calculated as a solution of the scattering equations (3.19) vs the comparative solution of the Maxwell equations (4.1) in a one-dimensional geometry for a homogeneous medium with a slab geometry shown in Fig. 1(a). The graphs are plotted as a function of detuning $\Delta = \omega - \tilde{\omega}_0$ from the displaced resonance frequency $\tilde{\omega}_0 = \omega_0 - \mu_c/\hbar$ (see the text). The results are performed for different sample depths L, scaled by the wavelength λ_0 at the atomic resonance, and for the density $n_0\lambda_0^3 \sim 0.05$. The reflection spectra for different L are unresolved in the graph with the plotted precision. The inset shows the dielectric permittivity of the sample $\epsilon(\omega) = \epsilon'(\omega) + i\epsilon''(\omega)$ given by solution of Eq. (3.17) as a function of $\omega - \omega_0$. Both the rounds of calculations give identical results, and to show this in the example of $L = 10\lambda_0$ we additionally indicate (by the dotted curve) the prediction of the macroscopic Maxwell theory.

tions by expanding $\sqrt{\epsilon(z,\omega)}$ in a Taylor series near the vacuum point $\epsilon = 1$ and keeping only the forwardly propagating wave in the macroscopic Maxwell description of the problem. Again the calculations show good (within the made approximations) agreement between both approaches. We used the same peak density $n_0\lambda_0^3 \sim 0.05$ and the same sample depths as in the plots of Fig. 2. In the case of smoothed sample bounds with a density profile $n_0(z) = n_0\cos^2(\pi z/L)$ the backward scattering is expected to be a many orders of magnitude weaker process because of vanishing boundary contributions. The latter can be seen via the negligible response of the reflected light as follows from the calculation data shown in the bottom panel of Fig. 3 and clarified in its inset.

B. Interference of two counterpropagating BEC fragments

Finally, let us consider the experimental configuration when, as a result of coherent interaction with light, a BEC
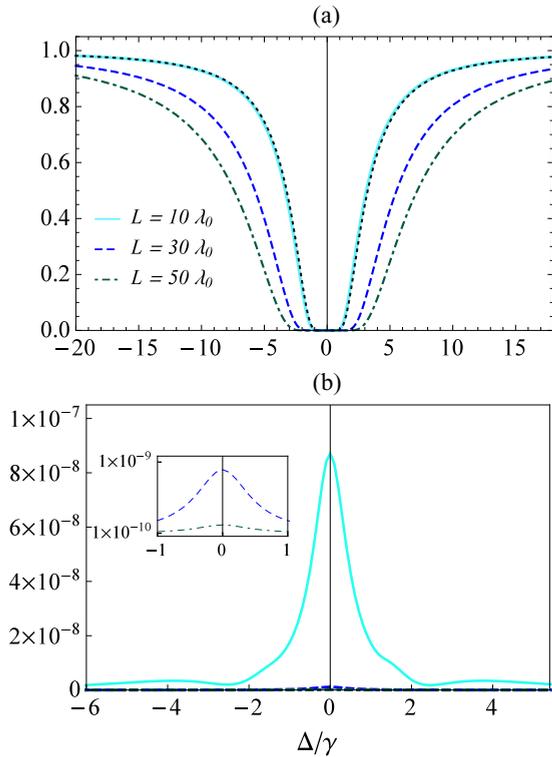
FIG. 3. Same as in Fig. 2 but for the density distribution parametrized by the order parameter $\Xi(z) = \sqrt{n_0} \cos(\pi z/L)$ for a slab geometry shown in Fig. 1(b). In the case of a smooth sample boundary the backward scattering reveals a many orders of magnitude weaker process than in the case of sharp boundaries.

sample is fractured into a number of macroscopic pieces [5,6]. To simplify the complicated experimental picture we model the process by the presence of only two fragments counterpropagating with respect to each other in their center-of-momentum reference frame. The considered configuration is shown in Fig. 1(c) and reveals a strong density oscillation associated with interference of the order parameters (matter wave packets) from the BEC pieces in the area of their overlapping. The existence of such a fringe structure of the density distribution has been directly observed as an effect of interference of two condensates in experiment [33]. The spatial phase-matching condition, determined by internal relative motion of the fragments, crucially affects the scattering process. Indeed, the wavelength of the oscillation is determined by the speed of relative motion and after accumulation of essential linear momentum from light can exceed a scale of the light wavelength. Then such a density grating should lead to strong Bragg diffraction and, as we show by our numerical simulations below, to significant enhancement of the backward scattering.

The process can be described by the order parameter of the spatial profile

$$\Xi(z) = \sqrt{2n_0} \cos\left(\frac{\pi z}{L}\right) \cos(\Delta q z)$$

$$= \sqrt{\frac{n_0}{2}} \cos\left(\frac{\pi z}{L}\right) e^{i\Delta q z} + \sqrt{\frac{n_0}{2}} \cos\left(\frac{\pi z}{L}\right) e^{-i\Delta q z}$$

$$\equiv \Xi_+(z) + \Xi_-(z), \qquad (4.2)$$

which is constructed as an ideal overlap of two matter wave packets associated with the condensate fragments of identical shape and size counterpropagating with respect to each other with the relative linear momentum $2\hbar\Delta q$ per atom. Let us make a clarifying comment concerning the validity and consistency of the suggested profile as a solution of the time-dependent Gross-Pitaevskii equation.

Both of the partial contributions $\Xi_+(z)$ and $\Xi_-(z)$ are representative solutions of the order parameter equation, for example, in the Thomas-Fermi approximation. That can be justified via transforming the dynamical description of any of the wave packets to that reference frame where the particular fragment is motionless and then we arrive at the configuration considered in the preceding section. However, the entire process of expansion and fragmentation of the condensate, modeled by (4.2), can be imagined only after the BEC is released from the trap and it results from both the external disturbance and internal interaction processes. The superposed state (4.2) can physically model the complicated dynamics of the condensate fragmentation once we ignore the weak nonideality of the atomic gas in comparison with the kinetic energy associated with the relative motion of the fragments [see the inequality (2.11)]. This can be fulfilled for quite high relative speed with $\Delta q \gg 1/L$ and $2\hbar^2\Delta q^2/m_A > \mu_c$. Then the factor $\cos(\Delta q z)$ is a strongly oscillating function of z, which implies its averaging $\langle \cos^2 \Delta q z \rangle \to 1/2$ in the normalization of the order parameter by a total number of particles. Then the expansion (4.2) corresponds to the beginning of the splitting process of the released matter wave $\Xi(z) = \sqrt{n_0} \cos(\pi z/L)$, as shown in Fig. 1(c), in two separated wave packets $\Xi_+(z)$ and $\Xi_-(z)$ propagating in opposite directions.

In Fig. 4 we show the spectra of transmission and reflection for the order parameter with the spatial profile given by Eq. (4.2). It is expected that for a classical disordered gas any internal motion of its macroscopic fragments with a rather slow relative speed would not modify the scattering process at all. As an example, such an expansion with a relative speed given by the recoil limit $\sim \hbar k_0/m_A$ would induce only a negligible Doppler shift between the spectral outputs from both fragments. However, in the case of BEC such an internal motion dramatically modifies the scattering process. As pointed out above, the spatial modulation of the order parameter initiates a mechanism of the Bragg diffraction and scattering on the spatially oscillating density. As a consequence, this leads to strong enhancement of the backward scattering and it is manifestable in an abrupt structure of the transmission spectrum as well. The strongest scattering is observed for the modulation wave number $\Delta q = k_0$ when the condensate expands with the relative speed $v_0 = 2\hbar k_0/m_A$. As follows from the dependences of Fig. 4, this effect experiences a broader spectral domain as the sample spatial scale is longer.

In Fig. 5 we reproduce the dependence of the reflection coefficient as a function of $2\pi/\Delta q$ for different sample depths L. As can be seen from these graphs, the reflection always has local maxima at the points $\Delta q = 2\pi/\lambda_0, 2\pi/2\lambda_0, \dots$. This is the optimal condition for manifestation of the Bragg diffraction, which creates the oppositely propagating polariton wave via scattering of the impinging wave on the periodic structure. As a consequence of the Bragg-type scattering, an additional amount of linear momentum transfers to the
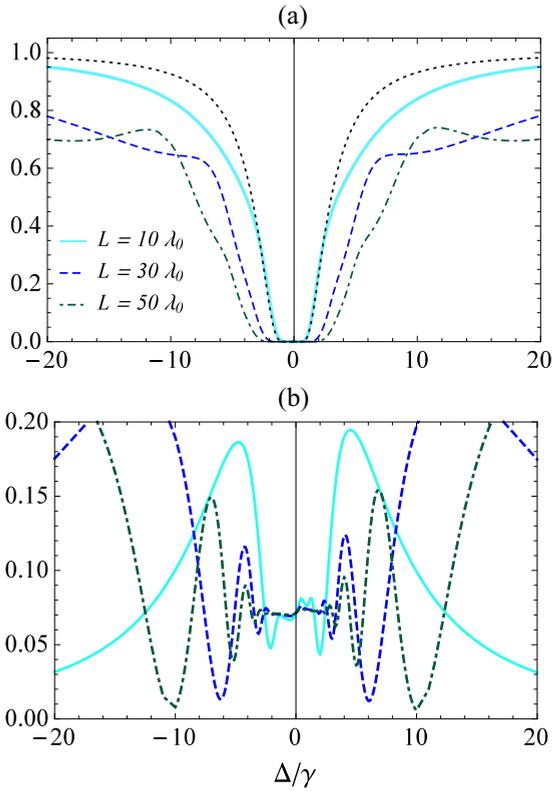
FIG. 4. Same as in Fig. 2 but for the density distribution parametrized by the order parameter $\Xi(z) = \sqrt{2n_0}\cos(\pi z/L)\cos(\Delta q z)$ with $2\Delta q = k_0$ for the geometry shown in Fig. 1(c). Both the forward and backward scattering have a clear signature of the coherent enhancement due to the effect of the Bragg diffraction. In (a) the dotted curve indicates the reference transmission spectrum for $L = 10\lambda_0$ with a smoothed profile of the order parameter and corresponds to the configuration of a disordered atomic gas.

condensate and enforces its fragmentation. So the Bragg diffraction also results in a certain optomechanical action on the system and accordingly leads to kinematic entanglement of the spatially structured BEC (see [6]).

In our calculation model we can describe such an effect of optomechanical interface primarily for the backward and
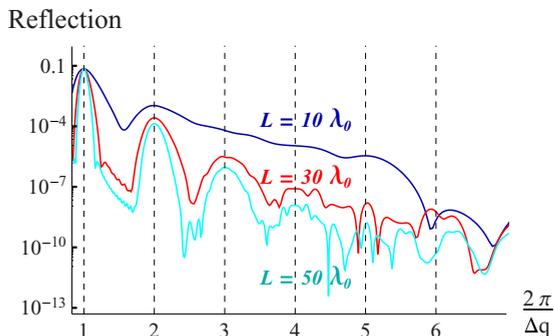

FIG. 5. Reflection coefficient for the order parameter of Fig. 4, at the point of atomic resonance, plotted as a function of $2\pi/\Delta q$ (in units of λ_0) for different sample depths L.

forward scattering channels. Nevertheless, in experiment [5] the fragmentation was observed for the scattering directions orthogonal to the incident light along the major axis of an ellipsoid-shaped condensate sample. The observed effect had been associated in [5] with the Kapitza-Dirac phenomenon of the matter wave scattering on the spatial structure created by an electromagnetic wave. In this sense, we can point out that in the case of excitation of a BEC sample by an external light pulse, consisting of many photons, the entire dynamics apparently results from several physical processes, which includes internal interactions, disturbance of the matter wave (order parameter) by an external driving field and formation of the polariton structure by optical excitation. Then the Bragg scattering reveals a coherent mechanism for rearranging photon-type polariton waves (see Sec. III C) propagating in different directions. The coherently scattered photons emerge from the sample, indicating the prior propagation directions of these waves.

V. CONCLUSION

In this paper we have developed a formalism of the microscopic quantum scattering theory directed towards an *ab initio* description of the elementary process of a single-photon scattering from a quantum degenerate atomic gas. The gas exists in the BEC phase parametrized by the order parameter introduced in the framework of the Gross-Pitaevskii model. The main mathematical objective of our calculational approach is the single-particle Green's function (propagator) tracking the propagation of a specific polariton wave through the condensate. The polariton is created as a quantum super-posed state between the photon and condensate.

The polariton propagation is disturbed by the process of incoherent scattering and its entire dynamics is described by the closed scattering equation for the complete polariton propagator as we derived. The crucial difference from the light propagation through a disordered nondegenerate atomic gas is that in the considered case the atomic medium represents a coherent matter wave strongly rejecting its classical interpretation. The conventional vision of the macroscopic Maxwell description of the electromagnetic wave in a bulk medium seems insufficient and even can be incorrect in some situations.

To clarify the above point we have solved the derived scattering equations in a one-dimensional geometry and compared the result with predictions of the conventional macroscopic Maxwell theory for the disordered atomic gas of the same density and size as the BEC sample. For steady-state conditions and uniform distribution of the order parameter we obtained identical results for the transmission and reflection spectra for both approaches. The most surprising seems the observation that excellent coincidence between the data has been obtained here from solutions of two different equations. From the point of view of the light scattering process, that nontrivially indicates physical equivalence between the classical-type disordered system, where atoms are randomly distributed as pointlike dipoles, and the uniform quantum coherent state, where atoms are distributed in the space as a matter wave expressed by a smooth profile of the order parameter. Such a quantum degenerate atomic system exists in a steady state

and can be associated with a relevant stationary solution of the Gross-Pitaevskii equation.

Nevertheless, we observe a significant difference once the BEC is fractured into a number of interfering matter wave fragments, which crucially modifies the density distribution. In the latter case the scattering process evolves towards conditions of Bragg diffraction, which strongly affects the process and can coherently redirect the propagating polariton wave in the backward or other directions associated with the condensate fragmentation. This type of Bragg diffraction is specific since the oscillating matter pattern is mostly sensitive to the relative speed of the fragments and can be observed even for low atomic densities. Evidently, such an usual density grating can be only phenomenologically performed under the frame of the conventional macroscopic Maxwell description and, as we pointed out, for a classical disordered gas any internal motion of its macroscopic fragments with a rather slow relative speed should not modify the scattering process at all.

APPENDIX A: OVERVIEW OF THE DIAGRAM APPROACH

Below we introduce basic elements of the diagram equations, which are constructed and discussed in the main text. We follow standard definitions and rules of the microscopic version of the Feynman diagram method, as described in Ref. [25], but revise it for a nonrelativistic dipole-type coupling of light and atoms (see Ref. [26]). The expansion of the evolution operator (2.10) in the Green's function (2.9) generates the sequence of expectation values of the various operator products, which after a set of transpositions and with the aid of the Wick theorem can be regrouped to the results visualized by diagrams. The diagrams consist of the objects given below.

The undisturbed causal-type electric-field Green's function is defined via transposition of the field operators in any pair product from chronologically T-ordered to normally N-ordered form

$$
\begin{aligned}
&i D_{\mu\mu'}^{(E)}(\mathbf{r},t;\mathbf{r}',t') \\
&= T\big[E_\mu^{(0)}(\mathbf{r};t)E_{\mu'}^{(0)}(\mathbf{r}';t')\big] - N\big[E_\mu^{(0)}(\mathbf{r};t)E_{\mu'}^{(0)}(\mathbf{r}';t')\big]. \quad \text{(A1)}
\end{aligned}
$$

It can be linked with a fundamental object of quantum electrodynamics, namely, with the causal-type photon propagator

$$
D_{\mu\mu'}^{(E)}(\mathbf{r},t;\mathbf{r}',t') = \frac{1}{c^2}\frac{\partial^2}{\partial t\,\partial t'}D_{\mu\mu'}^{(c)}(\mathbf{r},t;\mathbf{r}',t')\Big|_{\substack{\mathbf{r}\neq\mathbf{r}'\\ \text{or}\\ t\neq t'}}, \quad \text{(A2)}
$$

where we follow the gradient invariance of the theory and fix the propagator by a vanishing scalar potential such that $\mu,\mu' = x,y,z$. By simplifying the notation for each argument $\mu,\mathbf{r},t \to x$ and $\mu',\mathbf{r}',t' \to x'$, the electric-field Green's

function is imaged by a wavy line

$$
i D^{(E)}(x,x') \Leftrightarrow \quad \overset{\text{x}}{\sim\!\!\sim\!\!\sim\!\!\sim\!\!\sim}\overset{\text{x}'}{} \quad \text{(A3)}
$$

where the ending indices are often omitted in graph equations. This function depends only on the difference of its spatial and time arguments and its Fourier image is given by

$$
\begin{aligned}
D_{\mu\mu'}^{(E)}(\mathbf{k},\omega) &= \int d^3R \int_{-\infty}^{\infty} d\tau\, e^{i\omega\tau - i\mathbf{k}\cdot\mathbf{R}}\, D_{\mu\mu'}^{(E)}(\mathbf{R},\tau)\Big|_{\substack{\mathbf{R}=\mathbf{r}-\mathbf{r}'\\ \tau=t-t'}} \\
&= \frac{4\pi\hbar\omega^2}{\omega^2 - \omega_k^2 + i0}\left[\delta_{\mu\mu'} - c^2\frac{k_{\mu'}k_\mu}{\omega^2}\right], \quad \text{(A4)}
\end{aligned}
$$

where $\omega_k = ck$.

The electric-field Green's function is expressed via solution of the microscopic Maxwell equations with a pointlike dipole source and for $\omega > 0$ coincides with the positive-frequency component of the retarded-type fundamental solution of these equations $D_{\mu'\mu}^{(R)}(\mathbf{k},\omega)$,

$$
D_{\mu\mu'}^{(E)}(\mathbf{k},\omega)\big|_{\omega>0} = \frac{\omega^2}{c^2} D_{\mu\mu'}^{(R)}(\mathbf{k},\omega)\Big|_{\omega>0}. \quad \text{(A5)}
$$

The positive-frequency domain is only important in the RWA approach and in this approximation it is convenient to add an arrow in the diagram (A3) to indicate creation and annihilation events of a virtual photon at the edging points of the wavy line.

The undisturbed atomic Greens's function is defined via transposition of the atomic operators in any pair product from chronologically ordered to normally ordered form. For operators of the excited state this reads

$$
\begin{aligned}
&i G_{nn'}^{(0)}(\mathbf{r},t;\mathbf{r}',t') \\
&= T\big[\Psi_n^{(0)}(\mathbf{r};t)\Psi_{n'}^{(0)\dagger}(\mathbf{r}';t')\big] - \Psi_{n'}^{(0)\dagger}(\mathbf{r}';t')\Psi_n^{(0)}(\mathbf{r};t) \quad \text{(A6)}
\end{aligned}
$$

and similarly with the replacement $n,n' \to m = m' = 0$ for operators of the ground state. By simplifying the notation for each argument $n,\mathbf{r},t \to x$ and $n',\mathbf{r}',t' \to x'$ the atomic Green's function is imaged by an arrowed straight line

$$
i G^{(0)}(x,x') \Leftrightarrow \quad \overset{\text{x}}{\rule{3cm}{0.4pt}}\!\!\overset{}{<}\!\!\overset{\text{x}'}{\rule{0pt}{0pt}}\,, \quad \text{(A7)}
$$

where the ending indices are often omitted in graph equations. This function also depends only on the difference between its spatial and time arguments and its Fourier image is given by

$$
\begin{aligned}
G_{nn'}^{(0)}(\mathbf{p},E) &= \int d^3R \int_{-\infty}^{\infty} d\tau\, e^{(i/\hbar)E\tau - (i/\hbar)\mathbf{p}\cdot\mathbf{R}}\, G_{nn'}^{(0)}(\mathbf{R},\tau)\Big|_{\substack{\mathbf{R}=\mathbf{r}-\mathbf{r}'\\ \tau=t-t'}} \\
&= \delta_{nn'}\frac{\hbar}{E - p^2/2m_A - E_n + i0}, \quad \text{(A8)}
\end{aligned}
$$

where m_A is the atomic mass and the internal atomic state is assumed to be degenerate such that $E_n = \text{const}_n$.

The atomic Green's function is expressed by the fundamental solution (atomic propagator) of the Schrödinger equation for a free atom which describes propagation of an atomic wave initially localized in a certain spatial point. As follows from (A6), this function vanishes if $t < t'$ such that the

causal-type atomic propagator is identical to the retarded-type propagator.

There are different diagram vertices indicating optical interactions of different types. If a virtual photon interacts with an atom, which is also presented as a virtual object in a diagram, then in the RWA we associate the process with the two vertices

$$\frac{i}{\hbar} d_{nm}^\mu \quad \Leftrightarrow \quad \underset{n\quad m}{\longrightarrow\!\!\bullet\!\!\longleftarrow}^\mu ,$$

$$\frac{i}{\hbar} d_{mn}^\mu \quad \Leftrightarrow \quad \underset{m\quad n}{\longrightarrow\!\!\bullet\!\!\longleftarrow}^\mu . \tag{A9}$$

If a similar process is developing with condensate particles we associate it with the vertices of another type

$$\frac{i}{\hbar} d_{nm}^\mu \, \Xi(\mathbf{r}) \, e^{-\frac{i}{\hbar}\epsilon_0 t} \quad \Leftrightarrow \quad \underset{n\qquad\qquad\mu}{\longrightarrow\!\!\bullet\!\!\rightsquigarrow}^m ,$$

$$\frac{i}{\hbar} d_{mn}^\mu \, \Xi^*(\mathbf{r}) \, e^{+\frac{i}{\hbar}\epsilon_0 t} \quad \Leftrightarrow \quad \underset{\mu\qquad\qquad n}{\rightsquigarrow\!\!\bullet\!\!\longleftarrow}^m , \tag{A10}$$

which describe either excitation of an atom from the condensate phase (upper diagram) or its recovering in the condensate phase (lower diagram). The detailed specification of vertices is usually unnecessary and often omitted if it does not confuse interpretation of the diagram.

In the original representation each vertex corresponds to the integral over respective spatial and time variables and each contributing line is decoded in accordance with (A3) and (A7). In the stationary and homogeneous conditions after the Fourier transform, the external lines are decoded in accordance with (A4) and (A8) but internal lines, when they shape a loop, contribute as convolution-type integrals over reciprocal variables such as energy (frequency) and momentum (wave vector), with conservation of the total energy and momentum transporting by the diagram. For more details we refer the reader to Refs. [25,26].

APPENDIX B: ONE-DIMENSIONAL SCATTERING

Consider the scattering problem for a slab geometry of an atomic medium, homogeneous and infinite in the plane transverse to the wave vector of the incident photon. In this case the T-matrix element, given by Eq. (2.6) and selected for either forward or backward elastic scattering channels, is given by

$$T_{i'i}(E) = \frac{2\pi\omega}{\mathcal{L}} \iint dz' dz \sum_{n',n} (\mathbf{d}\cdot\mathbf{e})_{n'0}^* (\mathbf{d}\cdot\mathbf{e})_{0n}$$
$$\times e^{-ik'z'+ikz} \Xi^*(z')\Xi(z) G_{n'n}\big(z',z; E - E_0^{N-1}\big), \tag{B1}$$

where the output frequency and polarization are unchanged such that $\omega' = \omega$ and $\mathbf{e}' = \mathbf{e}$ and we redefined $f = i'$ with emphasis on the physical equivalence of initial and final states

in the one-dimensional scattering process. All the integrands are considered as functions of longitudinal coordinates z, z' and the polariton propagator is proportional to a δ function of transverse coordinates x, y and x', y' [see Eq. (3.19)]. The integral evaluated in the transverse plane over variables $dx\,dy$ and $dx'\,dy'$ cancels out the area scale $\mathcal{L}_x \mathcal{L}_y$ in the normalization volume $\mathcal{V} = \mathcal{L}_x \mathcal{L}_y \mathcal{L}_z$ and we defined $\mathcal{L}_z = \mathcal{L}$.

Let us express the S-matrix components via the T matrix

$$S_{i'i} = \delta_{i'i} - i\frac{\mathcal{L}}{\hbar c} T_{i'i}(E_i + i0). \tag{B2}$$

In a one-dimensional geometry for the nondegenerate ground state of the degenerate quantum gas the light scattering can be described by coefficients of transmission $\mathscr{T}(\omega)$, reflection $\mathscr{R}(\omega)$, and losses $\mathscr{L}(\omega)$, which are subsequently given by

$$\mathscr{T}(\omega) = |S_{i'i}|^2|_{k'=k>0}, \quad \mathscr{R}(\omega) = |S_{i'i}|^2|_{k'=-k<0},$$
$$\mathscr{L}(\omega) = 1 - \mathscr{T}(\omega) - \mathscr{R}(\omega) \tag{B3}$$

and can be found via solution of the simplified equations (3.19)–(3.21) as we show below.

Consider the example of the slab with the order parameter $\Xi(z) = \sqrt{n_0} = \mathrm{const}_z$ inside the medium. In this case the integral equation (3.19) can be transformed to the set of algebraic equations via spatial Fourier transform with periodic boundary conditions on the sample bounds. The azimuthal symmetry justifies the diagonal structure of the polariton propagator

$$G_{nn'}(z,z';E) = \delta_{nn'} G(z,z';E). \tag{B4}$$

Then, with the assumption that the origin of the coordinate frame is located in the middle point and $z \in (-L/2, L/2)$, where L is the sample length, it can be expanded as

$$G_{ss'}(E) = \frac{1}{L} \iint_{-L/2}^{L/2} dz\,dz'\, e^{-ik_s z + ik_{s'} z'} G(z,z';E),$$
$$G(z,z';E) = \frac{1}{L} \sum_{s,s'} e^{ik_s z - ik_{s'} z'} G_{ss'}(E), \tag{B5}$$

where $k_s = 2\pi s/L$ and $k_{s'} = 2\pi s'/L$ with $s, s' = 0, \pm 1, \pm 2, \ldots$. The Green's function (B4) contributes to the transmission amplitude (B2) at a specific energy argument $E - E_0^{N-1} = E_i - E_0^{N-1} = \hbar\omega + E_0^N - E_0^{N-1} = \hbar\omega + \varepsilon_0$ and we define

$$G_{ss'}(E)|_{E=\hbar\omega+\varepsilon_0} \equiv G_{ss'}(\omega) \tag{B6}$$

and consider the Fourier components as functions of the frequency of the incident photon. Then the S-matrix elements (B2) can be expressed as

$$S_{i'i} = \delta_{i'i} - \frac{8\pi i\omega}{L\hbar c} n_0 d_0^2 \sum_{s',s} \frac{\sin(k'-k_{s'})\frac{L}{2}}{k'-k_{s'}}$$
$$\times \frac{\sin(k-k_s)\frac{L}{2}}{k-k_s} G_{s's}(\omega), \tag{B7}$$

where $k = \omega/c$ and $k' = \pm\omega/c$.

By substituting (B4) and applying transforms (B5) to Eq. (3.19), considered in a one-dimensional configuration, we arrive at the system of algebraic equations

$$\left[\omega - \tilde{\omega}_0 + \frac{\hbar k_s^2}{2m_A} + \frac{4\pi}{3\hbar} n_0 d_0^2 + \frac{i}{2}\sqrt{\epsilon(\omega)}\gamma \right] G_{ss'}(\omega)$$
$$- \sum_{s''} \Sigma_{ss''}^{(c)}(\omega) G_{s''s'}(\omega) = \delta_{ss'}, \qquad (B8)$$

where $\tilde{\omega}_0 = (E_n - \varepsilon_0)/\hbar = (E_n - E_0 - \mu_c)/\hbar \equiv \omega_0 - \mu_c/\hbar$ with the same E_n for all upper state Zeeman sublevels. We approximated $\epsilon(\omega + \mu_c/\hbar) \approx \epsilon(\omega)$ [see Eq. (3.17) and the related comment].

The matrix of the self-energy part is given by

$$\Sigma_{ss}^{(c)}(\omega) = \frac{4\pi}{\hbar} n_0 d_0^2 \frac{\omega^2}{\omega^2 - c^2 k_s^2}$$
$$- \frac{4\pi i}{\hbar} n_0 d_0^2 \frac{\omega}{cL} \frac{\frac{\omega^2}{c^2} + k_s^2}{\left(\frac{\omega^2}{c^2} - k_s^2\right)^2} \left[1 - \exp\left(i\frac{\omega}{c}L\right) \right]$$
$$(B9)$$

for $s'' = s$ and

$$\Sigma_{ss''}^{(c)}(\omega) = -(-)^{s-s''} \frac{4\pi i}{\hbar} n_0 d_0^2 \frac{\omega}{cL} \frac{\frac{\omega^2}{c^2} + k_s k_{s''}}{\left(\frac{\omega^2}{c^2} - k_s^2\right)\left(\frac{\omega^2}{c^2} - k_{s''}^2\right)}$$
$$\times \left[1 - \exp\left(i\frac{\omega}{c}L\right) \right] \qquad (B10)$$

for $s'' \neq s$. For a sample of infinite length $L \to \infty$ Eqs. (B6) and (B8)–(B10) reproduce the transverse component of the polariton propagator in an infinite uniform medium [see Eq. (3.23)] and in this case the scattering process manifests itself mainly via the incoherent channels.

For the sample of finite length the system (B8) consists of an infinite number of equations. Nevertheless, it can be numerically solved with cutoff by a limited number of the involved equations. By increasing this number the iterative process becomes internally converging and approaches the exact solution. The performed calculation scheme can be straightforwardly generalized if the order parameter is nonuniform and described by trigonometric functions such as $\Xi(z) \sim \cos(\pi z/L)$ and $\Xi(z) \sim e^{i\kappa_1 z} \cos(\pi z/L) + e^{i\kappa_2 z} \cos(\pi z/L)$, which we have considered in our numerical simulations.

[1] H. D. Politzer, Phys. Rev. A **43**, 6444(R) (1991).

[2] M. H. Anderson, J. R. Ensher, M. R. Matthews, C. E. Wieman, and E. A. Cornell, Science **269**, 198 (1995).

[3] K. B. Davis, M.-O. Mewes, M. R. Andrews, N. J. van Druten, D. S. Durfee, D. M. Kurn, and W. Ketterle, Phys. Rev. Lett. **75**, 3969 (1995).

[4] S. Inouye, A. P. Chikkatur, D. M. Stamper-Kurn, J. Stenger, D. E. Pritchard, and W. Ketterle, Science **285**, 571 (1999).

[5] D. Schneble, Y. Torii, M. Boyd, E. W. Streed, D. E. Pritchard, and W. Ketterle, Science **300**, 475 (2003).

[6] A. Hilliard, F. Kaminski, R. le Targat, C. Olausson, E. S. Polzik, and J. H. Müller, Phys. Rev. A **78**, 051403(R) (2008); J. H. Müller, D. Witthaut, R. le Targat, J. J. Arlt, E. S. Polzik, and A. J. Hilliard, J. Mod. Opt. **63**, 1886 (2016).

[7] M. R. Matthews, B. P. Anderson, P. C. Haljan, D. S. Hall, C. E. Wieman, and E. A. Cornell, Phys. Rev. Lett. **83**, 2498 (1999).

[8] F. Chevy, K. W. Madison, and J. Dalibard, Phys. Rev. Lett. **85**, 2223 (2000).

[9] M. F. Andersen, C. Ryu, P. Cladé, V. Natarajan, A. Vaziri, K. Helmerson, and W. D. Phillips, Phys. Rev. Lett. **97**, 170406 (2006).

[10] J. F. S. Brachmann, W. S. Bakr, J. Gillen, A. Peng, and M. Greiner, Opt. Express **19**, 12984 (2011).

[11] M. G. Bason, R. Heck, M. Napolitano, O. Elíasson, R. Müller, A. Thorsen, W.-Z. Zhang, J. Arlt, and J. F. Sherson, arXiv:1607.02934.

[12] K.-P. Marzlin, W. Zhang, and E. M. Wright, Phys. Rev. Lett. **79**, 4728 (1997).

[13] J. E. Williams and M. J. Holland, Nature (London) **401**, 568 (1999).

[14] K. T. Kapale and J. P. Dowling, Phys. Rev. Lett. **95**, 173601 (2005).

[15] M. G. Moore and P. Meystre, Phys. Rev. Lett. **83**, 5202 (1999).

[16] O. Zobay and G. M. Nikolopoulos, Phys. Rev. A **73**, 013620 (2006).

[17] E. D. Trifonov, Laser Phys. **12**, 211 (2002).

[18] Y. A. Avetisyan and E. D. Trifonov, Phys. Rev. A **88**, 025601 (2013).

[19] Y. A. Avetisyan and E. D. Trifonov, Phys.-Usp. **58**, 286 (2015).

[20] N. N. Bogoliubov, J. Phys. (USSR) **11**, 23 (1947).

[21] L. P. Pitaevskii, Sov. Phys. JETP, **13**, 451 (1961) L.P. Pitaevskii [J. Exp. Theor. Phys. (USSR) **40**, 646 (1961)].

[22] E. P. Gross, Nuovo Cimento **20**, 454 (1961); J. Math. Phys. **4**, 195 (1963).

[23] V. M. Ezhova, L. V. Gerasimov, and D. V. Kupriyanov, J. Phys.: Conf. Ser. **769**, 012045 (2016).

[24] C. Cohen-Tannoudji, J. Dupont-Roc, and G. Grynberg, *Atom-Photon Interactions: Basic Processes and Applications* (Wiley, New York, 1992).

[25] V. B. Beresteskii, E. M. Lifshitz, and L. P. Pitaevskii, *Course of Theoretical Physics: Quantum Electrodynamics* (Pergamon, Oxford, 1981); E. M. Lifshitz and L. P. Pitaevskii, *Course of Theoretical Physics: Statistical Physics, Part II* (Pergamon, Oxford, 1980).

[26] D. V. Kupriyanov, I. M. Sokolov, and M. D. Havey, Phys. Rep. **671**, 1 (2017).

[27] I. M. Sokolov, M. D. Kupriyanova, D. V. Kupriyanov, and M. D. Havey, Phys. Rev. A **79**, 053405 (2009).

[28] J. Ruostekoski and J. Javanainen, Phys. Rev. A **56**, 2056 (1997).

[29] C. Salomon, G. Shlyapnikov, and L. F. Cugliandolo, *Many-Body Physics with Ultracold Gases* (Oxford University Press, Oxford, 2013).

[30] K. Levin, A. L. Fetter, and D. M. Stamper-Kurn, *Ultracold Bosonic and Fermionic Gases* (Elsevier, Oxford, 2012).

[31] L. D. Landau and E. M. Lifshitz, *Course of Theoretical Physics: Electrodynamics of Continuous Media* (Pergamon, Oxford, 1981).

[32] R. P. M. J. W. Notermans, R. J. Rengelink, and W. Vassen, Phys. Rev. Lett. **117**, 213001 (2016).

[33] M. R. Andrews, C. G. Townsend, H.-J. Miesner, D. S. Durfee, D. M. Kurn, and W. Ketterle, Science **275**, 637 (1997).